Identification of a short ACE2-derived stapled peptide targeting the SARS-CoV-2 Spike protein

Lorenzo Calugi, Giulia Sautariello, Elena Lenci, Andrea Trabocchi*

Department of Chemistry "Ugo Schiff", University of Florence, via della Lastruccia 13, 50019 Sesto Fiorentino, Florence, Italy

ABSTRACT: The design and synthesis of a series of peptide derivatives based on a short ACE2 α-helix 1 epitope and subsequent [i-i+4] stapling of the secondary structure resulted in the identification of a 9-mer peptide capable to compete with recombinant ACE2 towards Spike RBD in the micromolar range. Specifically, SARS-CoV-2 Spike inhibitor screening based on colorimetric ELISA assay and structural studies by circular dichroism showed the ring-closing metathesis cyclization being capable to stabilize the helical structure of the 9-mer [34]HEAEDLFYQ[42] epitope better than the triazole stapling via click chemistry. The results are preliminary for the development of small molecule stapled peptides capable of blocking the key ACE2-Spike S1 protein-protein interaction.

The Respiratory Syndrome caused by Coronavirus SARS-CoV-2 that appeared at the end of 2019[1,2] has put in serious difficulty the health systems globally and raised health concerns as well as unprecedented economic challenges. The restriction measures that were necessary to counteract the spread of the contagion have caused serious losses to the economies and the budget for health has significantly increased to allow the recovery of a high number of people mainly through hospitalization in intensive care units. As of April 2022, the COVID-19 outbreak has been responsible for over 500 million infections and 6 million confirmed deaths worldwide.[3] While the introduction of vaccines (11 billion vaccine doses administered)[3] has made it possible to keep most acute infections under control (0.1% serious and critical cases among 68 million actually infected people, as of April 2022)[4], it is also true that immunosuppressed or unvaccinated subjects still represent an easily attackable target, in particular with the onset of new and potentially more contagious and infectious genetic variants of SARS-CoV-2 that continue to emerge and spread.[5] If mass vaccination represents an excellent emergency response, a normal situation would only have positive aspects to be drawn from the presence of targeted treatments to counter the effects of lung infection in infected subjects without the need of expensive treatments such as intubation and hospitalization in intensive care.

To date, a series of therapies are being implemented for the treatment of COVID-19,[6] and drug classes currently used include antiviral agents, inflammation inhibitors, antirheumatic drugs, plasma and therapeutic antibodies. Given the nature of the coronavirus, the greatest efforts are focused on key events linked to the infection, the blocking of the Spike-ACE2 (angiotensin-converting enzyme 2) interaction and the inhibition of the viral proteins necessary for replication, such as the 3CLPro protease[7,8] and the RNA-dependent RNA polymerase (RdRp).[9] The first process represents the initial contact between the virus and the host cells to promote fusion with the host cell membrane for subsequent release of the genetic material necessary for viral replication.

The viral entry for SARS-CoV-2 is a key event mediated by the Spike transmembrane protein that forms homotrimers, each structure consisting of a S1 subunit that binds to ACE2 of the host cell via a receptor-binding domain (RBD) to initiate infection, a S2 subunit that mediates virus fusion with host cells, and a transmembrane domain. The RBD-Spike S1-ACE2 protein-protein interaction at the surface of epithelial cells has been identified as the molecular event causing the infection of human respiratory cells.[10-13] Given the pivotal role of such proteins for promoting viral entry and replication, SARS-CoV-2 monoclonal antibodies (mAbs) have been developed successfully for their capability to bind to the spike receptor-binding domain of the SARS-CoV-2, preventing viral entry into host cells, taking advantage of high specificity that limits their "off-target" toxicity, although showing reduced antiviral potency with the occurrence of viral variants.[14] Complimentary to this therapeutic approach, small molecule entry inhibitors impairing virus particles from infecting human cells could be used to prevent SARS-CoV-2 infection and to shorten the outcome of COVID-19 infections.

The structure and characterization of the ACE2-fragment S1 complex of the SARS-CoV-2 spike protein obtained with the cryo-EM technique was soon reported (Figure 1, left),[15,16] allowing to identify the structural determinants responsible for protein-protein interaction, particularly those involving the spike RBD directly interacting with the exposed domain of ACE2 consisting of the *N-* and *C*-terminal regions of the helix α1 and small areas of the helix α2 (Figure 1, right).
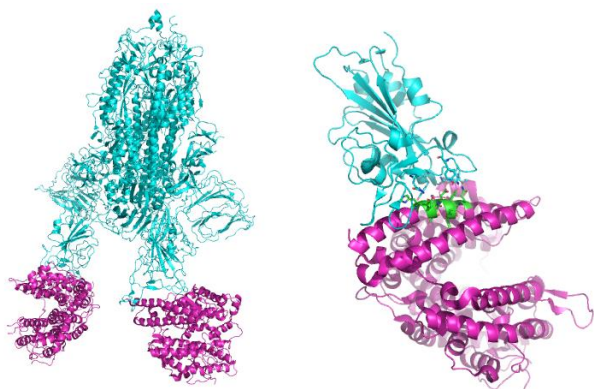
Figure 1. Left: trimeric Spike protein (cyan) complexed to two ACE2 fragments (purple, PDB: 7A97); right: close-up of RBD (cyan)-ACE2 (purple) interaction and highlight of the selected ACE2 α-helix 1 epitope (green, PDB: 6M0J).

Specifically, the central segment of ACE2 α-helix 1 is involved in strong interactions mainly engaging polar residues. At the N-terminal end of α-helix 1, Y41, Q42 and D38 experience a hydrogen bond network with Q498, T500 and N501 spike residues, whereas in the middle of the α-helix 1 bridge, H34 interacts with Y453 of spike RBD. In this view, A36, L39 and F40 in this helical epitope are not directly involved in the interaction with the spike binding region (Figure 2).
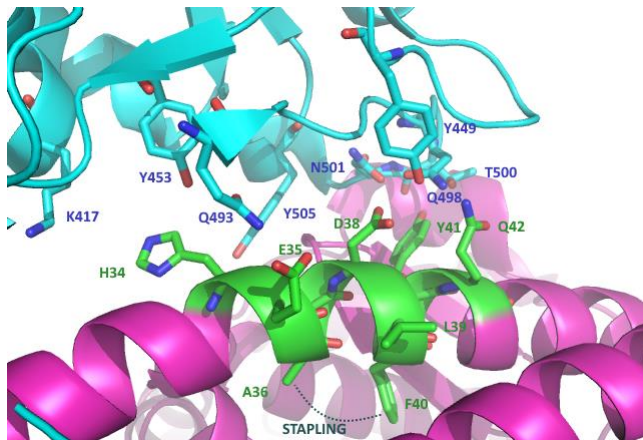
Figure 2. Magnification of RBD (cyan)-ACE2 (purple) interaction, highlighting the selected ACE2 α-helix 1 epitope (green, PDB: 6M0J), the key interacting amino acids and the selected amino acids for the [i – i+4] stapling region.

Taking advantage of such structural biology data published with unprecedented speed, several research groups considered the structure-based design of peptides and stapled constructs as mimetics of ACE2 α-helix 1 motif, capable of disrupting the key Spike RBD-ACE2 protein-protein interaction. The absence of binding pockets as hot spots in this PPI that develops on a rather extensive surface made the identification of small molecule PPI inhibitors rather difficult.[17,18]

Based on the structure of the RBD-ACE2 complex, a first-in-class 23-mer peptide capable of binding RBD with nanomolar affinity according to interferometry bio-layer experiments was reported.[19] Successively, Karoyan et al. developed a ACE2-derived 27-mer mimetic of the N-terminal of the α-helix

1, capable of binding the Spike RBD with IC$_{50}$ in the nM range as measured by ELISA test, and suggesting a potential application as a nasal or oral spray to overcome the limited biodistribution and bioavailability of peptides.[20]

Starting from the evidence of peptidomimetics as promising and more druggable inhibitors of PPIs,[21,22] stapled peptidomimetics of the ACE2 α-helix 1 were proposed to block the bioactive helical conformation using chemical linkers. Peptide stapling increases the helicity in solution of small unstructured peptides, improves resistance against proteolysis, increases potency and often improves cell penetration.[23-29] Accordingly, Mecinović et al. reported the synthesis of 35-mer stapled peptides based on ACE2 α-helix 1 displaying μM activity in ELISA based screening assays. Debnath and collab., based on the α-helix 1 and the identified key interactions, designed 30-mer peptides with double stapling that showed a high percentage of helicity and the capability to inhibit the activity of SARS-CoV-2 through *in vitro* pseudovirus and viral infectivity assays. Interestingly, the less active compounds showed a sequence with the key Q42 being replaced with an alkenyl amino acid useful for the stapling.[31] Similarly, Jamieson et al. reported a stapling array of 10- to 23-mer α-helix 1 ACE2 peptidomimetics.[32] Although possessing the helix structure in solution, as confirmed by circular dichroism, none of them showed activity in fluorescence polarization and neutralization assays.

In view of developing short peptidomimetics capable of acting as entry inhibitors, we got interested in the work by Larue and collab.[33] that rationally designed and tested a series of small peptide inhibitors of the Spike-ACE2 interaction, based on the minimal conserved 6-mer [37]EDLFYQ[42] epitope of ACE2 α-helix 1 interacting domain, resulting in the identification of two peptides possessing mM inhibition potency towards SARS-CoV-2 infection. Starting from this epitope, we devised selecting the longer 9-mer [34]HEAEDLFYQ[42] epitope to introduce a minimal [i – i+4] stapling and maintaining Q42 as the C-terminal amino acid, following the observation that the presence of the two following serine residues ([43]SS[44]) in the peptide may affect the peptide flexibility and activity, as reported.[33] From the structural data on the Spike RBD-ACE2 interaction (Figure 2) the two amino acids A36 and F40 were identified for the stapling region, due to their orientation at the opposite site of the helix interacting with the RBD and at the right distance for the [i – i+4] helix pitch (Figure 2).

All the peptides were synthesized using a microwave-assisted solid-phase synthesis protocol.[31,34] The peptide epitope [34]HEAEDLFYQ[42] and its *N*-acetyl derivative were synthesised as reference compounds (Table 1). Briefly, the peptides were synthesized using a ChemMatrix Rink Amide resin, with a 0.5 mmol/g loading capacity. DIC/Oxyma[35] was used as the activating mixture for coupling Fmoc-amino acids, and morpholine was used as a Fmoc deblocking agent. 95% TFA containing water and TIPS as scavengers, each in 2.5% amount was used as the cleaving mixture. Peptides were precipitated using cold diethyl ether and purified by reverse-phase HPLC and characterized by analytical HPLC and ESI-MS.

Table 1. Sequence and inhibitory activity of selected ACE2 epitopes and peptidomimetics.[a]

Entry	Sequence/Structure	Yield, %	% inhib. at 30 μM
1	H-HEAEDLFYQ-NH$_2$	28	20
2	Ac-HEAEDLFYQ-NH$_2$	39	12
3		46	6
4		12	30
5		35	8
6		15	55 (21±7 μM)[b]
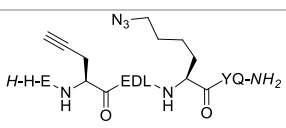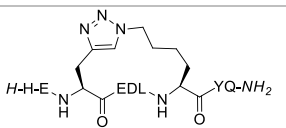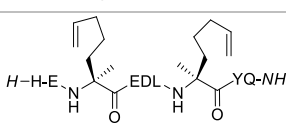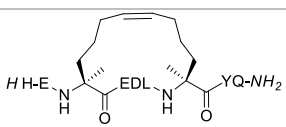
[a] Mean from three different assays, errors were in the range of 5-10% of the reported values

[b] IC$_{50}$ value was retrieved from dose-response assays as the concentration of compound required for 50% inhibition and estimated by non-linear correlation using GraphPad Prism software.

The stapling between A36 to F40 was achieved using both click chemistry[36] and ring-closing metathesis (RCM)[31,37] on solid-phase. The linear peptide precursors **3** and **5** were synthesised as controls (Table 1). The formation of a triazole through the Cu-catalyzed azide-alkyne cycloaddition (CuAAC) reaction as a click chemistry approach was achieved by replacing A36 with Fmoc-Pra-OH (Fmoc-propargyl-Gly-OH) and F40 with Fmoc-Lys(N$_3$)-OH (Fmoc-azidolysine) in the peptide sequence. The fully protected resin-bound peptide was treated with CuBr and sodium ascorbate in a DMF/DMSO mixture containing DIPEA and 2,6-Lutidine, and stirring the resin for 5 min at room temperature and then under microwave irradiation at 55 °C for 10 min. After final Fmoc deprotection and peptide cleavage, subsequent purification *via* semi-preparative HPLC allowed to obtain peptide **4** in 12% overall yield. For the synthesis of the stapled peptide via RCM the two amino acids A36 and F40 were replace with the quaternary amino acid Fmoc-(*S*)-2-(4-pentenyl)Ala-OH. The metathesis was carried out on the fully protected resin-bound peptide, too, using 1st generation Grubbs catalyst (15 mg for 0.05 mmol resin-bound peptide) in 1,2-dichloroethane. After final Fmoc deprotection and peptide cleavage, subsequent purification by semi-preparative HPLC allowed to obtain peptide **6** in 15% overall yield.

The synthesized compounds were tested to verify their biological activity using a competitive ELISA assay, which measures the binding of the RBD of the Spike protein from SARS-CoV-2 to its human receptor ACE2 (Table 1). The SARS-CoV-2 inhibitor in the samples competes with ACE2 to combine with immobilized SARS-CoV-2 spike RBD. The signal colour becomes lighter as the content of SARS-CoV-2 inhibitor increases. Concerning the selected peptide epitope **1** and the *N*-acetyl derivative **2**, the competitive ELISA assay at 30 μM concentration did not show a significant inhibition of the spike RBD-ACE2 interaction with respect to biotinylated ACE2. Concerning stapled peptides with respect to the linear precursors, a significant inhibitory activity was observed for the RCM stapled peptide **6**, whereas the triazole-stapled peptide **4** showed minor activity, even though better than the corresponding linear precursor **3** and the reference peptide **1**. The RCM stapling as in **6** allowed to constrain the peptide epitope in the bioactive conformation, taking advantage of the two quaternary amino acids as the stapling elements, capable of promoting a higher degree of helicity and providing a flexible tether for the modulation of the conformation to the bioactive shape. A dose-response assay was carried out for **6** to achieve a inhibition curve of SARS-CoV-2 Spike Protein (RBD) in the range of 10 nM–300 μM, resulting in a IC$_{50}$ value of 21 μM, thus suggesting the importance of RCM stapling to improve the inhibition potency of a minimal ACE2 epitope (Figure 3).
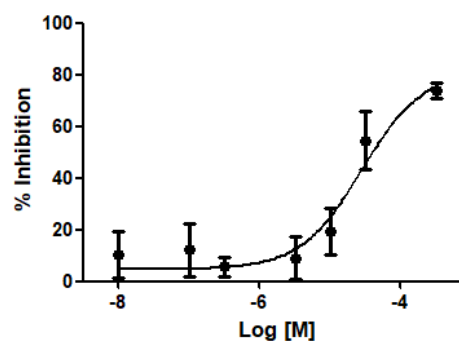
Figure 3. Inhibition curve of **6** on Spike RBD-ACE2 interaction.

Circular dichroism analyses were performed in the range from 190 nm to 250 nm on peptides **4**, **6** and the corresponding linear precursors **3** and **5** as PBS solutions at a concentration of 500 and 100 μM to determine the secondary structure of the peptides in PBS buffer (Figure 4). Both stapled peptides **4** and **6** exhibited an appreciable α-helix degree. On the other hand, the linear precursor **3** of the stapled triazole peptide **4** showed a spectrum attributable to random coil. The unexpected result obtained for the linear peptide **5** was attributed to the presence of disubstituted α,α-amino acids that recall the structure of α-aminoisobutyric acid, already widely characterized as a helicity inducer in linear peptides.[38] Nevertheless, such helical character of **5** was not sufficient to achieve a significant binding to RBD.
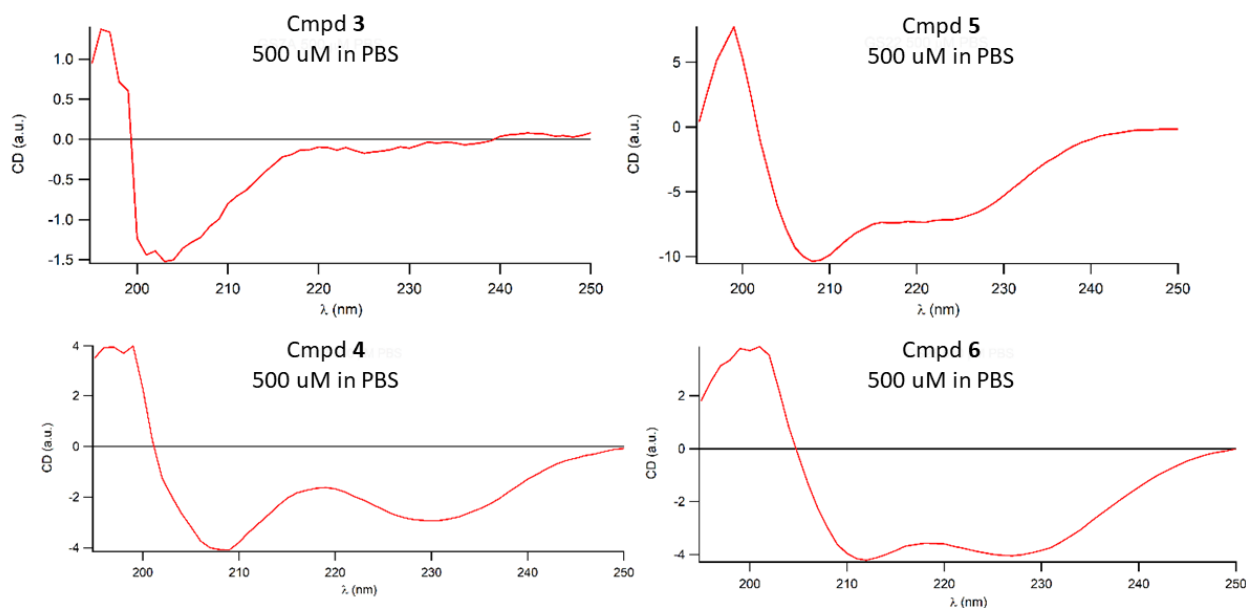
Figure 4. Circular dichroism spectra of triazole-stapled peptide **4** and RCM-stapled peptide **6** along with linear precursors **3** and **5**, respectively, at 500 µM in PBS. Spectra were recorded between 190 and 250 nm.

In conclusion, the synthesis of short stapled peptides based on a α-helix 1 ACE2 epitope was achieved, resulting in the identification of a RCM-stapled 9-mer peptide capable to compete with recombinant ACE2 towards Spike RBD in the micromolar range, according to competitive ELISA assay on immobilized SARS-CoV-2 Spike RBD. Structural studies by circular dichroism showed RCM cyclization being capable to stabilize the helical structure better than triazole stapling via click chemistry, also taking advantage of quaternary amino acids promoting peptide helicity. The results are preliminary for the development of a small molecule stapled peptide capable of interfering with the key ACE2-Spike S1 protein-protein interaction.

Experimental Section

All commercially available reagents and solvents were used as received. Solid-phase peptide synthesis was carried out using an automated single-mode microwave synthesizer (Initiator Sixty, Biotage AB) using sealed reaction vessels and built-in internal pressure and temperature sensors. HPLC analyses were performed on synthesized peptides using Dionex Ultimate 3000 system. ESI-MS were carried out on methanol/formic acid solutions by direct inlet on a LCQ Fleet™ Ion Trap LC/MS system (Thermo Fisher Scientific) using electrospray (ES+ or ES-) ionization techniques. The spectra of **6** were obtained in 4 mM 90% HDO where aggregation was not significant. TOCSY-ES spectra were recorded with 80 ms mixing time, 2048 points in t1, 400 points in t2, and 32 scans per t2 increment.

- General procedure for peptide synthesis

The peptides were synthesized on the ChemMatrix Rink Amide resin, with a 0.5 mmol/g loading capacity and bead size of 100-200 mesh. Peptide cleavage from the resin was achieved under acidic conditions. The resin was swelled in dichloromethane (DCM) for 20 min, under magnetic stirring prior to peptide synthesis. Then, the solution was filtered and washed twice with *N,N*-dimethylformamide (DMF). Peptide coupling were carried out using 5 eq. the Fmoc-amino acids as 0.2 M DMF solution and 10 eq. DIC/Oxyma, both 1M in DMF as the activating mixture by heating at 90 °C for 3 min, followed by DMF washings (x3). 20% Morpholine was used as Fmoc deblocking agent by heating at 90 °C for 2 min (x2), each cycle followed by DMF washings (x3). Final resin washing before acidic cleavage were carried out with DMF (x3) and CH_2Cl_2 (x2). A mixture of 2.5% H_2O and 2.5% TIPS in TFA was added into the peptidyl resin, and the suspension was shaken for 2 h followed by filtration. Cold diethyl ether (10 mL) was added to the filtrate, and peptide was precipitated. The mixture was centrifuged for 3 min at 2500 rpm, and the ether layer was separated. The procedure was repeated three times, then a second treatment with TFA containing water and TIPS was repeated for 15 min, followed by peptide precipitation with cold ether. Then, the peptide was dried under vacuum overnight to give the crude peptide.

- HPLC Purification and analysis

Peptides were analyzed and purified using Dionex Ultimate 3000 system equipped with a reverse-phase analytical column Synergi 4 µm Fusion-RP 80 Å (150 x 4.6 mm) or semi-preparative column Synergi 10 µm Fusion-RP 80 Å (250 x 10.0 mm) and using acetonitrile (0.1% TFA) in H_2O (0.1% TFA) at

room temperature, 5-95% linear gradient over 20 min for analytical and semi-preparative runs or alternatively 5-30%/3', 30-50%/27' and 50-95%/2' as gradient for semi-preparative runs. A flow rate of 1 and 5 mL/min were used for analytical and semi-preparative runs, respectively, and peak detection was achieved at 223 nm. All crude peptides were obtained in >95% purity. The molecular weight of all peptides was confirmed by electrospray mass spectrometry. Analytical samples were prepared as 1 mg/mL conc. by dissolving the dry peptides in 0.1% H_2O/HCOOH (v/v).

- *Compound* 1. The linear peptide **1** was achieved in 28% yield using 100 mg of ChemMatrix Rink Amide resin and following the general procedures for peptide synthesis and HPLC purification. HPLC: 90% purity, rt = 10.36 min; ESI-MS: *m/z* 1151.20 [M+H]$^+$.

- *Compound* 2. The linear peptide **2** was achieved in 39% yield using 100 mg of ChemMatrix Rink Amide resin and following the general procedures for peptide synthesis and HPLC purification. Acetylation of the *N*-terminal amino acid was carried out on solid phase using a DMF solution of Ac_2O (20 eq) and DIPEA (20 eq) for 30 min at room temperature. HPLC: 95% purity, rt = 10.65 min; ESI-MS: *m/z* 1192.31 [M+H]$^+$.

- *Compound* 3. The linear peptide **3** was achieved in 46% yield using 100 mg of ChemMatrix Rink Amide resin and following the general procedures for peptide synthesis and HPLC purification. Fmoc-Pra-OH (Fmoc-propargyl-Gly-OH) and Fmoc-Lys(N_3)-OH were used in *i* and *i*+4 relative positions in place of Ala and Phe of the reference peptide **1**, respectively. HPLC: 92% purity, rt = 10.22 min; ESI-MS: *m/z* 1179.43 [M-H]$^-$.

- *Compound* 4. The triazole-stapled peptide **4** was achieved in 12% yield using 100 mg of ChemMatrix Rink Amide resin and following the general procedures for peptide synthesis and HPLC purification. Fmoc-Pra-OH (Fmoc-propargyl-Gly-OH) and Fmoc-Lys(N_3)-OH were used in *i* and *i*+4 relative positions in place of Ala and Phe of the reference peptide **1**, respectively. The cyclization was carried out on resin and before the deprotection of the last Fmoc-amino acid. In a test tube, Cu(I)Br and sodium ascorbate were dissolved in a DMF/DMSO, then DIPEA and 2,6-Lutidine were added. This solution was then transferred to the reactor containing the peptide resin and nitrogen was bubbled into the mixture for 5 min at room temperature and then heated under microwave irradiation at 55 °C for 10 min, followed by resin washing by DMF (x2), CH_2Cl_2 (x2) and DMF (x2). Final Fmoc deprotection and peptide cleavage from the resin was carried out as described in the general procedure for peptide synthesis. HPLC: 99% purity, rt = 8.64 min; ESI-MS: *m/z* 1181.47 [M+H]$^+$.

- *Compound* 5. The linear peptide **5** was achieved in 35% yield using 100 mg of ChemMatrix Rink Amide resin and following the general procedures for peptide synthesis and HPLC purification. Fmoc-(*S*)-2-(4-pentenyl)alanine was used in *i* and *i*+4 relative positions in place of Ala and Phe of the reference peptide **1**. HPLC: 89% purity, rt = 12.27 min; ESI-MS: *m/z* 1210.41 [M+H]$^+$.

- *Compound* 6. The RCM-stapled peptide **6** was achieved in 15% yield using 100 mg of ChemMatrix Rink Amide resin and following the general procedures for peptide synthesis and HPLC purification. Fmoc-(*S*)-2-(4-pentenyl)alanine was used in

i and *i*+4 relative positions in place of Ala and Phe of the reference peptide **1**. The cyclization was carried out on resin and before the deprotection of the last Fmoc-amino acid. Initially, the resin was washed 3 times with CH_2Cl_2. Then 5 mL (maximum capacity of the reactor used) of 1,2-dichloroethane (DCE) in the reactor and the solution was bubbled with nitrogen. After 15 min, 15 mg (amount for 0.05 mmol resin-bound peptide) of 1st-generation Grubbs catalyst was added and the solution was bubbled with nitrogen for 4 h. Then, the solution was filtered, and the resin was successively washed with MeOH (x2), CH_2Cl_2 (x2) and MeOH (x2). Final Fmoc deprotection and peptide cleavage from the resin were carried out as described in the general procedure for peptide synthesis. HPLC: 94% purity, rt = 11.67 min; ESI-MS: *m/z* 1181.50 [M-H]$^-$.

- *Circular dichroism spectroscopy*

Selected peptide molecules were analyzed with respect to the secondary structure by means of circular dichroism spectroscopy (CD). The spectra were acquired at the Jasco j-810 spectropolarimeter, in the range from 190 nm to 250 nm. Samples were prepared at a concentration of 500 and 100 μM in phosphate-buffered saline (PBS).

- *SARS-CoV-2 Spike/hACE2 Inhibitor Screening Assays*

The synthesized peptides were screened for inhibition of the SARS-CoV-2 Spike/hACE2 complex formation using a commercially available SARS-CoV-2 Spike Inhibitor Screening Assay Kit (AdipoGen Life Sciences, Inc., San Diego, USA) based on the colorimetric ELISA assay, which measures the binding of the RBD of the Spike S protein from SARS-CoV-2 to its human receptor ACE2. All the measurements were performed in triplicates in 96-well plates following the manufacturer's instructions. Briefly, the wells were coated by adding 100 μL/well of diluted SPIKE (1 μg/mL) to the 96-well ELISA microplate. After leaving the covered plate overnight at 4 °C, the liquid was removed by the wells by inverting the plate and blotting it against clean absorbent paper. Then, the plate was blocked by adding 200 μL of blocking buffer for 2 h at room temperature. Following liquid removal and washing of coated wells, 100 μL/well of diluted compounds to be tested were added to the wells and the plate covered and incubated for 1 h at 37 °C. 100 μL/well of inhibitory control ACE2 (human) mAb was used as a positive control. Then, 100 μL/well of diluted HRP labeled streptavidin was added and the plate covered and incubated again for 1 h at room temperature. After liquid removal and subsequent washings, substrate development was conducted by addition of 100 μL of ready-to-use TMB to each well for 5 min at room temperature, then the reaction was stopped by adding 50 μL of Stop Solution, the OD values measured at 450 nm using a BMG Labtech Fluostar Optima microplate reader and the collected data were analyzed using Graphpad 5.0 Software Package (Graphpad Prism, San Diego, CA). All the compounds were screened for inhibition at a single concentration (30 μM) in PBS, and the IC$_{50}$ value of the active compound was obtained by dose-response measurements using inhibitor range of concentration 0.01–300 μM.

SUPPLEMENTARY MATERIAL

Copies of HPLC chromatograms and ESI-MS spectra of **1**-**6**, copies of ^{1}H-ES and TOCSY-ES of **6**.

AUTHOR INFORMATION

* Corresponding Author

Andrea Trabocchi – Department of Chemistry "Ugo Schiff", University of Florence, via della Lastruccia 13, I-50019 Sesto Fiorentino, Florence, Italy; orcid.org/0000-0003-1774-9301; Email: andrea.trabocchi@unifi.it

REFERENCES

[1] Zhou, P., Yang, X. L., Wang, X. G., Hu, B., Zhang, L., Zhang, W., Si, H. R., Zhu, Y., Li, B., Huang, C. L., et al. (2020) A pneumonia outbreak associated with a new coronavirus of probable bat origin. *Nature* 579, 270–273.

[2] Wu, F., Zhao, S., Yu, B., Chen, Y. M., Wang, W., Song, Z. G., Hu, Y., Tao, Z. W., Tian, J. H., Pei, Y. Y., et al. (2020) A new coronavirus associated with human respiratory disease in China. *Nature* 579, 265–269

[3] WHO, Coronavirus disease (COVID-19) Pandemic, https://www.who.int/emergencies/diseases/novel-coronavirus-2019, accessed April 5th 2022

[4] Worldometer, Coronavirus Cases, https://www.worldometers.info/coronavirus/coronavirus-cases/#daily-cases, accessed April 5th 2022

[5] Callaway, E. (2021) Beyond Omicron: what's next for COVID's viral evolution. *Nature* 600, 204–207

[6] Robinson, P. C., Liew, D. F. L., Tanner, H. L., Grainger, J. R., Dwek, R. A., Reisler, R. B., Steinman, L., Feldmann, M., Ho, L. -P., Hussell, T., Moss, P., Richards, D., Zitzmann, N. (2022) COVID-19 therapeutics: Challenges and directions for the future. *Proc. Natl. Acad. Sci. U.S.A.* 119, e2119893119

[7] Qiu, Y., Xu, K. (2020) Functional studies of the coronavirus nonstructural proteins. *STEMedicine* 1, e39

[8] Vandyck, K., Deval, J. (2021) Considerations for the discovery and development of 3-chymotrypsin-like cysteine protease inhibitors targeting SARS-CoV-2 infection. *Curr. Opin. Virol.* 49, 36–40

[9] Painter, G. R., Natchus, M. G., Cohen, O., Holman, W., Painter, W. P. (2021) Developing a direct acting, orally available antiviral agent in a pandemic: the evolution of molnupiravir as a potential treatment for COVID-19. *Curr. Opin. Virol.* 50, 17–22

[10] Xiu, S., Dick, A., Ju, H., Mirzaie, S., Abdi, F., Cocklin, S., Zhan, P., Liu, X. (2020) Inhibitors of SARS-CoV-2 Entry: Current and Future Opportunities. *J. Med. Chem.* 63, 12256–12274

[11] Hoffmann, M., Kleine-Weber, H., Schroeder, S., Krüger, N., Herrler, T., Erichsen, S., Schiergens, T. S., Herrler, G., Wu, N. -H., Nitsche, A., Müller, M. A., Drosten, C., Pöhlmann, S. (2020) SARS-CoV-2 Cell Entry Depends on ACE2 and TMPRSS2 and Is Blocked by a Clinically Proven Protease Inhibitor. *Cell* 181, 271–280.e8

[12] Jackson, C. B., Farzan, M., Chen, B., Choe, H. (2021) Mechanisms of SARS-CoV-2 entry into cells. *Nat. Rev. Mol. Cell Biol.* 1–18

[13] Letko, M., Marzi, A., Munster, V. (2020) Functional assessment of cell entry and receptor usage for SARS-CoV-2 and other lineage B betacoronaviruses. *Nat. Microbiol.* 5, 562–569

[14] Taylor, P.C., Adams, A.C., Hufford, M.M. de la Torre, I., Winthrop, K., Gottlieb, R. L. (2021) Neutralizing monoclonal antibodies for treatment of COVID-19. *Nat. Rev. Immunol.* 21, 382–393

[15] Yan, R., Zhang, Y., Li, Y., Xia, L., Guo, Y., Zhou, Q. (2020) Structural basis for the recognition of SARS-CoV-2 by full-length human ACE2. *Science* 367, 1444-1448

[16] Benton, D. J., Wrobel, A. G., Xu, P., Roustan, C., Martin, S. R., Rosenthal, P. B., Skehel, J. J., Gamblin, S. J. (2020) Receptor binding and priming of the spike protein of SARS-CoV-2 for membrane fusion. *Nature* 588, 327-330

[17] Sheng, C., Dong, G., Miao, Z., Zhang, W., Wang, W. (2015) State-of-the-art strategies for targeting protein-protein interactions by small-molecule inhibitors *Chem. Soc. Rev.* 44, 8238-8259

[18] Geppert, T., Hoy, B., Wessler, S., Schneider, G. (2011) Context-based identification of protein-protein interfaces and "hot-spot" residues. *Chem. Biol.* 18, 344-353

[19] G. Zhang, S. Pomplun, A. R. Loftis, A. Tan, A. Loas, B. L. Pentelute (2020) Investigation of ACE2 N-terminal fragments binding to SARS-CoV-2 Spike RBD. *bioRxiv* 2020.03.19.999318.

[20] Karoyan, P., Vieillard, V., Gómez-Morales, L., Odile, E., Guihot, A., Luyt, C. -E., Denis, A., Grondin, P., Lequin, O. (2021) Human ACE2 peptide-mimics block SARS-CoV-2 pulmonary cells infection. *Commun. Biol.* 4, 197

[21] Lenci, E., Trabocchi, A. (2020) Peptidomimetic toolbox for drug discovery. *Chem. Soc. Rev.* 49, 3262-3277

[22] Ali, A. M., Atmaj, J., Van Oosterwijk, N., Groves, M. R., Dömling, A. (2019) Stapled Peptides Inhibitors: A New Window for Target Drug Discovery. *Comput. Struct. Biotechnol. J.* 17,263-281

[23] Charoenpattarapreeda, J., Tan, Y. S., Iegre, J., Walsh, S. J., Fowler, E., Eapen, R. S., Wu, Y., Sore, H. F., Verma, C. S., Itzhaki, L., Spring, D. R. (2019) Targeted covalent inhibitors of MDM2 using electrophile-bearing stapled peptides. *Chem. Commun.* 55, 7914-7917

[24] Dougherty, P. G., Wen, J., Pan, X., Koley, A., Ren, J. G., Sahni, A., Basu, R., Salim, H., Appiah Kubi, G., Qian, Z., Pei, D. (2019) Enhancing the Cell Permeability of Stapled Peptides with a Cyclic Cell-Penetrating Peptide. *J. Med. Chem.* 62, 10098-10107

[25] Cowell, J. K., Teng, Y., Bendzunas, N. G., Ara, R., Arbab, A. S., Kennedy, E. J. (2017) Suppression of Breast Cancer Metastasis Using Stapled Peptides Targeting the WASF Regulatory Complex. *Cancer Growth Metastasis.* 10, 1179064417713197

[26] Dietrich, L., Rathmer, B., Ewan, K., Bange, T., Heinrichs, S., Dale, T. C., Schade, D., Grossmann, T. N. (2017) Cell Permeable Stapled Peptide Inhibitor of Wnt Signaling that Targets β-Catenin Protein-Protein Interactions. *Cell Chem. Biol.* 24, 958-968.e5

[27] Gaillard, V., Galloux, M., Garcin, D., Eléouët, J. F., Le Goffic, R., Larcher, T., Rameix-Welti, M. A., Boukadiri, A., Héritier, J., Segura, J. M., Baechler, E., Arrell, M., Mottet-Osman, G., Nyanguile, O. (2017) A Short Double-Stapled Peptide Inhibits Respiratory Syncytial Virus Entry and Spreading. *Antimicrob. Agents Chemother.* 61, e02241-16

[28] Cromm, P. M., Spiegel, J., Grossmann, T. N. (2015) Hydrocarbon stapled peptides as modulators of biological function. *ACS Chem. Biol.* 10, 1362-1375

[29] Verdine, G. L., Hilinski, G. J. (2012) Stapled peptides for intracellular drug targets. *Methods Enzymol.* 503, 3-33

[30] Maas, M. N., Hintzen, J. C. J., Löffler, P. M. G., Mecinović, J. (2021) Targeting SARS-CoV-2 spike protein by stapled hACE2 peptides. *Chem. Commun.* 57, 3283-3286

[31] Curreli, F., Victor, S. M. B., Ahmed, S., Drelich, A., Tong, X., Tseng, C. K., Hillyer, C. D., Debnath, A. K. (2020) Stapled Peptides Based on Human Angiotensin-Converting Enzyme 2 (ACE2) Potently Inhibit SARS-CoV-2 Infection In Vitro. *mBio* 11, e02451-20

[32] Morgan, D. C., Morris, C., Mahindra, A., Blair, C. M., Tejeda, G., Herbert, I., Turnbull, M. L., Lieber, G., Willett, B. J., Logan, N., Smith, B., Tobin, A. B., Bhella, D., Baillie, G., Jamieson, A. G. (2021) Stapled ACE2 peptidomimetics designed to target the SARS-CoV-2 spike protein do not prevent virus internalization. *Pept. Sci.* e24217

[33] Larue, R. C., Xing, E., Kenney, A. D., Zhang, Y., Tuazon, J. A., Li, J., Yount, J. S., Li, P. -K., Sharma, A. (2021) Rationally Designed ACE2-Derived Peptides Inhibit SARS-CoV-2. *Bioconj. Chem.* 32, 215–223

[34] Pedersen, S. L., Tofteng, A. P., Malik, L., Jensen, K. J. (2012) Microwave heating in solid-phase peptide synthesis. *Chem. Soc. Rev.* 41, 1826-1844

[35] Subirós-Funosas, R., Prohens, R., Barbas, R., El-Faham, A., Albericio, F. (2009) Oxyma: an efficient additive for peptide synthesis to replace the benzotriazole-based HOBt and HOAt with a lower risk of explosion. *Chem. Eur. J.* 15, 9394-9403

[36] D'Ercole, A., Sabatino, G., Pacini, L., Impresari, E., Capecchi, I., Papini, A. M., Rovero, P. (2020) On-resin microwave-assisted copper-catalyzed azide-alkyne cycloaddition of H1-relaxin B single chain 'stapled' analogues. *Pept. Sci.* 112, e24159

[37] Barragán, F., Moreno, V., Marchán, V. (2009) Solid-phase synthesis and DNA binding studies of dichloroplatinum(ii) conjugates of dicarba analogues of octreotide as new anticancer drugs. *Chem. Commun.* 31, 4705-4707

[38] Biondi, B., Casciaro, B., Di Grazia, A., Cappiello, F., Luca, V., Crisma, M., Mangoni, M. L. (2017) Effects of Aib residues insertion on the structural-functional properties of the frog skin-derived peptide esculentin-1a(1-21)NH2. *Amino Acids* 49, 139-150